ELSEVIER

Biochimica et Biophysica Acta 1195 (1994) 259–266

BBA Biochimica et Biophysica Acta

Design of a short membrane-destabilizing peptide covalently bound to liposomes

Christophe Puyal [a,*], Luc Maurin [a], Geneviève Miquel [b], Alain Bienvenüe [a], Jean Philippot [a]

[a] *URA 530 CNRS Interactions Membranaires, Dépt. Biologie-Santé, CP 107, Université des Sciences et Techniques du Languedoc, F-34095 Montpellier Cédex 5, France*

[b] *URA 330 CNRS, BP 5051, route de Mende, F-34033 Montpellier Cédex, France*

Received 15 April 1994

Abstract

We characterized the physical and biological properties of a 14-residue amphipathic sequence called SFP (for short fusogenic peptide). At acidic pH, this short synthetic peptide interacts with various phospholipidic monolayers. These interactions were correlated with a pH-dependent conformational transition of SFP resulting in a hydrophobic α-helical structure. The hemolysis assay showed a pH-dependent weak membrane destabilizing activity of SFP. However, membrane anchoring of SFP through a covalently bound myristic acid enhanced by 1000-fold its membrane-destabilizing power. Moreover, SFP covalently bound to fluorescent-labeled liposomes induced a pH-dependent mixing of both membranes. SFP, a small synthetic peptide, is thus able to mimick many aspects of viral protein-induced membrane fusion: conformational change, membrane destabilization, membrane anchoring and finally pH-dependent lipid mixing.

Keywords: Fusogenic peptide; Monolayer; Liposome

1. Introduction

Membrane fusion is a widespread and ubiquitous process essential for cell physiology and virus infectivity [1,2]. Although the molecular mechanism is still poorly understood, there are many common points between inter- or intra-cellular and viral fusion processes, particularly concerning the involvement of fusion proteins. Virus infectivity is one of the most studied fusion processes [3]. Virus-induced fusion is mediated by one or several combined specific proteins [4]. Viral proteins show common characteristics, especially the presence of a 'fusion peptide' [5]. Fusion peptide sequences are short, relatively hydrophobic and always associated with a membrane-anchored subunit [6]. Current evidence strongly indicates that fusion peptides interact with the lipid environment of the target membrane before membrane destabilization [7,8]. This interaction requires a conformational change in the fusion protein leading to an organized secondary structure of the fusion peptide [9–11].

Our aim was to design a drug vector analogous to the F-protein liposome [12] but with lower immunogenicity [13] and endowed with a fusogenic pH-dependent peptide. First, we selected the peptide required to induce membrane fusion. This choice was based on the sequence, length and peptide membrane binding. The rationale for the sequence design was threefold, it had: (1) to be short, capable of insertion in one single monolayer in order to destabilize the bilayer membrane, (2) to have a pH-induced conformational change creating well separated hydrophilic and hydrophobic faces, and finally, (3) to be able to covalently bind to a membrane.

It was previously shown that GALA, a 30-residue amphipathic peptide with a repeat unit of glutamic acid-alanine-leucine-alanine, interacts with and destabilizes uncharged lipid bilayers in a pH-dependent fashion [14]. This was correlated with a pH-induced random coil–α transi-

Abbreviations: chol, cholesterol; DMF, dimethyl formamide; DOPC, 1,2-dioleoyl-*sn*-glycero-3-phosphocholine; MA, myristic acid; NBD, 7-nitrobenz-2-oxa-1,3-diazol-4-yl; NBD-PE, phosphatidylethanolamine labeled at the amino group with NBD; PC, phosphatidylcholine; PE, phosphatidylethanolamine; PS, phosphatidylserine; RET, resonance energy transfer; Rh, rhodamine; Rh-PE, phosphatidylethanolamine labeled at the amino group with lissamine rhodamine B sulfonyl; SFP, short fusogenic peptide; SMCC, *N*-succinimidyl 4-(*N*-maleimidomethyl)cyclohexane-1-carboxylate; Tes, *N*-tris[hydroxymethyl]methyl-2-aminoethanesulfonic acid (2-([2-hydroxy-1,1-bis(hydroxymethyl)ethyl]amino)ethanesulfonic acid); Tris, tris(hydroxymethyl)aminomethane.

* Corresponding author. Fax: +33 67 144286.

SSDI 0005-2736(94)00199-5

tion [15]. In helical conformation, GALA was designed to have an alignment of hydrophilic (Glu) and hydrophobic (Leu) residues on opposing faces [16], facilitating interactions with membranes. This synthetic peptide is of great interest due to its ability to mimick some features of fusogenic peptides from viral fusion proteins. However, GALA has always been used in solution and has never been anchored into a membrane until now [15].

In this paper, we investigated the destabilizing and fusogenic capability of a 14-residue GALA-type peptide (SFP for short fusogenic peptide) and the importance of its prior membrane-anchoring.

2. Materials and methods

2.1. Materials

The protected amino acids and the PepSyn KA type resin used for the peptide synthesis were obtained from Neosystem and Millipore, respectively. Bovine brain phosphatidylserine (PS), egg-yolk phosphatidylcholine (PC), 1,2-dioleoyl-*sn*-glycero-3-phosphocholine (DOPC), egg-yolk phosphatidylethanolamine (PE), 1,2-dihexadecanoyl-*rac*-glycero-3-phosphoethanolamine (DPPE), cholesterol (chol) and tetradecanoic acid (myristic acid, MA) were purchased from Sigma. ^{3}H-Myristic acid was obtained from Amersham. *N*-Succinimidyl 4-(*N*-maleimidomethyl)cyclohexane-1-carboxylate (SMCC) was obtained from Pierce. *N*-(Lissamine rhodamine B sulfonyl)diacylphosphatidylethanolamine (Rh-PE) and *N*-(7-nitrobenz-2-oxa-1,3-diazol-4-yl)diacylphosphatidylethanolamine (NBD-PE) were obtained from Molecular Probes. All other reagents and chemicals were of analytical grade.

2.2. Peptide synthesis

Three GALA-type peptides were synthesized: SFP-1 with the amino acid sequence F-E-A-A-L-A-E-A-L-A-E-A-L-A; SFP-2 with the same sequence as SFP-1 but with an NH_2-terminal myristic acid (MA) derivatization; and SFP-3 with the sequence W-E-A-A-L-A-E-A-L-A-E-A-L-A-C. These peptides were synthesized via their C-terminal extremity by solid-phase synthesis on a Milligen 9050 continuous flow peptide synthesizer using fluoren-9-methoxycarbonyl (Fmoc) chemistry and a polyacrylic type resin (PepSyn KA, Millipore). The dual-coupling method was used to increase the coupling yield. Maximum coupling times were 1 h, and the final peptide was cleaved by treatment with trifluoroacetic acid/phenol/water/ethanedithiol/thioanisol (9.2:0.2:0.2:0.2:0.2, v/v) at room temperature for 2 h. After trifluoroacetic acid (TFA) vacuum-evaporation, the peptide was precipitated three times by addition of a large volume of freezing diethyl ether and then filtered through a polytetrafluoroethylene membrane (FA filter type, Millipore) with 1 μm pore size. The peptide was then dissolved in 1% ammonia and purified by reverse-phase HPLC (Waters, Millipore) using a semi-preparative Delta Pak 7.8 × 300 mm column with 15 μm/C_{18}-300 Å characteristics (Waters, Millipore) at a flow rate of 1 ml/min with two continuous gradients: 30–80% B over the first 10 min; then 80–95% over the last 5 min (B = 99.92% acetonitrile/0.08% TFA; A = 99.9% water/0.1% TFA).

For SFP-2, tritiated MA was added in the last step of synthesis and in the same excess as the amino acids just before peptide cleavage from the resin. Radioactivity counts were done to follow the derivatized peptide during HPLC purification and characterization. DMF was the most convenient solvent to dissolve the peptide in non-aggregated form before HPLC purification.

For SFP-3, a Cys was added to the C-terminal extremity to couple the peptide to liposomes via a maleimide-functionalized PE (SMCC-PE) obtained synthetically. A Trp was used instead of Phe_1 of SFP-1 or SFP-2 to be able to detect the peptide by fluorescence.

Purity and identity of the peptides were confirmed by HPLC (Waters 486, Millipore), amino acid analysis, and fast atom bombardement mass spectroscopy (FAB-MS) on a trio 2000 mass spectrometer (VG Biotech). The peptides were stable for up to 2 months when stored as a lyophilized powder at −20°C under argon.

2.3. Peptide hydrophobicity

To evaluate hydrophobicity of the peptide at different pH, the phase-partitioning measurement between the aqueous phase (citrate-phosphate buffer) and 1-octanol was performed. SFP-1 was taken as a 1 mM stock solution in 200 mM disodium hydrogen phosphate at pH 8.8 and diluted into the appropriate buffer (10 mM acetate, 150 mM NaCl (pH 5.0) or 10 mM Tes, 150 mM NaCl (pH 7.5)) to obtain a 0.2 mM solution. An equal volume (500 μl) of 1-octanol was then added. The mixture was strongly vortexed for 3 min. After phase partitioning, the amount of remaining peptide was determined by the method of Lowry et al. [17] in a 200-μl aliquot from the aqueous phase.

2.4. Monolayer measurements

Monolayer experiments were performed at 18°C in a thermostatically controlled box. The surface pressure at the air/water interface was measured using the Wilhelmy plate method [18] and a home-built film balance [19]. Experiments were performed at constant area using a 50-ml teflon trough, 6 cm in diameter. The subphase consisted of twice distilled water, once on potassium permanganate. The pH of the subphase was continuously monitored with a combined glass microelectrode and adjusted to the desired value with microinjections of 1 M ammonium hydroxide or 1 M acetic acid under magnetic stirring. 20 to 100 μl of lipid stock solutions in chloroform

(about 0.1 mg/ml) was spread at the air/water interface using a small glass capillary. The peptide was added to the subphase through a small hole drilled at the edge of the trough using a Hamilton syringe, and the resulting change in surface pressure was recorded until a constant equilibrium value was reached.

2.5. Circular dichroism experiments

The CD spectra of SFP-1 were recorded at different pH levels on a Jobin Yvon Dichrograph V spectropolarimeter. The spectra were scanned in quartz suprasil cells with a 10 mm path length. The spectral domain was between 190 and 250 nm. All experiments were performed at 25°C. SFP-1 was taken as a 1 mg/ml stock solution in 0.5% ammonia at pH 8.0 and was diluted into degassed citrate-phosphate buffer so as to obtain a 0.1 mg/ml peptide solution at the desired pH. There was no citrate phosphate buffer absorption in the UV range. All θ values are expressed as deg cm^2 $dmol^{-1}$.

Since Subbarao et al. [16] have shown that interpretations of GALA spectra below 222 nm in the presence of phospholipid vesicles are ambiguous and the helical content of many peptides is known to be increased in interactions with lipids [9,20,21], no CD measurement was done in the presence of lipid vesicles.

2.6. Hemolysis assay

The hemolysis assay was performed according to the modified procedure of Schlegel and Waden [22]. Fresh human whole blood collected on ACD (85 mM trisodium citrate, 111 mM glucose, 71 mM citric acid (pH 7.4)) was obtained from a blood bank (Centre Régional de Transfusion Sanguine, Montpellier, France). Prior to use, erythrocytes were isolated by washing the blood three times in isotonic solution (150 mM NaCl) followed by resuspension in the appropriate buffer (A: 10 mM acetate, 150 mM NaCl (pH 5.0); B: 10 mM Tes, 150 mM NaCl (pH 7.4)) at 10^8 cells/ml. Assays were performed in 1 ml total volume samples. Isotonic stock solutions of tested molecules (SFP-1, SFP-2 or myristic acid) were mixed at different final concentrations with the human erythrocyte suspension. The mixture was then transferred to a 37°C water bath for 10 min under gentle stirring and centrifuged at 4°C for 30 s at $3000 \times g$. Hemolysis was measured by supernatant absorbance at 541 nm (spectrophotometer Uvikon 930, Kontron Instruments). Total hemolysis was estimated by lysing 10^8 cells in 1.0 ml of distilled water. Spontaneous hemolysis of erythrocytes representing less than 5% of total hemolysis was subtracted from the experimental values.

2.7. Preparation of liposomes

Two kinds of liposomes were prepared by probe sonication of an egg PC/chol/SMCC-PE (6:3:0.5) mixture, supplemented with either NBD-PE or Rh-PE at a fluorescent probe/total lipid molar ratio of 1:100. Briefly, the lipids in chloroform/methanol solutions were mixed and dried under nitrogen followed by high vacuum for 2 h. Lipid films were dispersed in 20 mM Tris/150 mM NaCl (pH 7.4) and sonicated for 14 min with a 50% active cycle on a Vibra Cell (Bioblock) at 4°C under argon. This procedure yields liposomes with a diameter of about 200 nm. Electron microscopy (Jeol 1 200) confirmed the liposome size estimated by photon correlation spectroscopy (N4S sub-micron particle analyzer, Coultronics) and showed an apparent size homogeneity with a low level of multilamellar liposomes ($< 4\%$). SMCC-PE is dipalmitoylphosphatidylethanolamine derived with SMCC, a heterobifunctional crosslinker, according to the coupling procedure with SPDP [23].

The peptide (SFP-3) was conjugated to liposomes via reaction of SFP-3 thiol group with the liposome maleimide group. SFP-3 was dissolved in 20 mM ammonium bicarbonate (pH 8.0). Fivefold excess of SFP-3 versus the maleimide group was added to vesicles and incubated at 4°C for 20 h. The liposomes were collected after centrifugation ($160\,000 \times g$) through a two-step dextran gradient (20; 10%). After lipid phosphorus measurement [24], the final lipid concentration was 1 mM. The coupling yield (10–20%) was determined by tryptophan fluorescence intensity ($\lambda_{ex} = 280$ nm; $\lambda_{em} = 348$ nm). Finally, synthetic fusogenic liposomes contained a peptide/total lipid ratio of 1:400.

2.8. Lipid mixing assay

SFP-induced vesicle fusion, as assayed by lipid mixing, was monitored using resonance energy transfer (RET) between NBD and Rh probes. Briefly, 50-μl aliquots of each preparation of fluorophore-labeled liposomes were diluted with 1.9 ml of 20 mM Tris/150 mM NaCl (pH 7.4). A pH of 4.5 was obtained by injection of 8 μl of 1 M HCl. Fluorescence emission spectra (500–650 nm) were monitored with a SLM Aminco fluorometer ($\lambda_{ex} = 470$ nm). Intermixing of lipids of the two vesicle populations led to a decrease in the NBD fluorescence signal (λ_{530}) concomitant with an increase in the Rhodamine fluorescence signal (λ_{590}). Fusion is shown by an increase in energy transfer efficiency occurring when probes are mixed within the same membrane [25].

3. Results

3.1. Peptide hydrophobicity

As the hydrophobicity of fusion peptides is an important parameter in the fusion process, the hydrophobic character of SFP-1 was determined using the phase partition method. As shown in Fig. 1, hydrophobicity of SFP-1

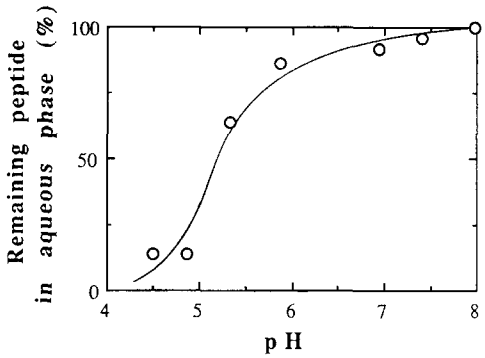

Fig. 1. Percent of SFP-1 remaining in the aqueous phase after phase-partition as a function of pH. An equal volume of 1-octanol was added to a 0.2 mM SFP-1 in citrate-phosphate buffer at the appropriate pH.

was strongly pH-dependent with an apparent pK_a between 5 and 5.5. Indeed, at pH lower than 5, only 10% of the total peptide was retained in the aqueous phase. This observation suggested that strong peptide–phospholipid interactions should be observed at acidic pH.

3.2. Peptide insertion into lipid monolayers

Since the lipid monolayer system simulates one side of a bilayer structure, we used this attractive model to study interactions between SFP-1 and lipid targets. The ability of a peptide to interact with a lipid substrate can be determined by the corresponding increase in surface pressure of the lipid monolayer, at constant surface area. A significant surface pressure increase is interpreted as being a consequence of the insertion of the hydrophobic portion of the peptide into the hydrophobic part of the lipid monolayer.

In preliminary experiments without lipid film (data not shown), SFP-1 was injected into the aqueous phase and its adsorption behaviour was followed at the air/water interface as a function of pH. Reduction of the surface tension was only observed at acidic pH (the equilibrium spreading pressure was around 10 mN/m), confirming the strong pH dependence of the hydrophobicity of SFP-1.

Subsequently, the pH profile of the surface activity of SFP-1, (10 μM final concentration) was determined in the presence of a DOPC monolayer. As shown in Fig. 2, there was no modification in the surface pressure at basic and neutral pH. On the contrary, SFP-1 showed substantial surface activity at acidic pH (leading to a surface pressure increase of 12.8 mN/m at pH 4.8), with an apparent pK_a of about 5.5. The kinetics of SFP-1-induced surface activity reached a plateau within a few minutes after a rapid increase in $\Delta\Pi$ (Fig. 2, inset).

To evaluate the involvement of the charge density and the nature of the polar headgroups in these interactions, surface pressure variations at pH 4.8 were performed following the addition of SFP-1 under three different lipid monolayers (DOPC, PE and PS monolayers) at various initial surface charge densities and initial pressures (Π_i) (see Fig. 3). The affinity of peptides to lipid surfaces is currently evaluated by measuring the exclusion pressure (Π_e) (where a peptide is unable to penetrate or interact with the lipid film). Π_e was determined by extrapolating the surface pressure increase to zero [7]. $\Delta\Pi$ is a linear function of Π_i, as previously described for fusogenic peptides [26]. For initial surface pressures of less than 20 mN/m, no substantial difference was observed between DOPC, PE and PS monolayers. The exclusion pressures of SFP-1 in DOPC, PS and PE monolayers were, respectively, 29, 33 and 36 mN/m, indicating a marked capacity of the peptide to penetrate into the membrane. Additional experiments were performed with a pure peptide film and showed a collapse pressure of around 22 mN/m. This value was lower than the critical pressure of insertion, demonstrating the miscibility of both compounds in the surface layer. However, beyond the initial pressure of 20 mN/m, a biphasic curve shape was obtained with the DOPC monolayer, revealing a particular affinity of SFP-1 to DOPC. All the dots represent means of three different experiments. The maximum difference between two values was lower than 0.5 mN/m. Interestingly, when SFP-1 was injected beneath a monolayer of PC/chol (2:1, molar ratio) or PC/PS/chol (1:1:1, molar ratio), the plateau observed with the pure DOPC monolayer was never obtained (Fig. 3, inset).

From this set of data, we conclude that the lipid charge density was not a major requirement for the interaction between SFP-1 and the monolayer. Szoka and coll. [16] pointed out the shielding effect of the ionic strength on GALA glutamic carboxylate anions. In our experiments, the (SFP-1)-induced surface pressure increases with a DOPC monolayer were not affected by the addition of sodium chloride up to 200 mM (data not shown).

To determine whether the surface pressure increase was actually connected with penetration of SFP-1 into the phospholipid monolayer and not simply due to adsorption, the reversibility of the phenomenon was studied. The

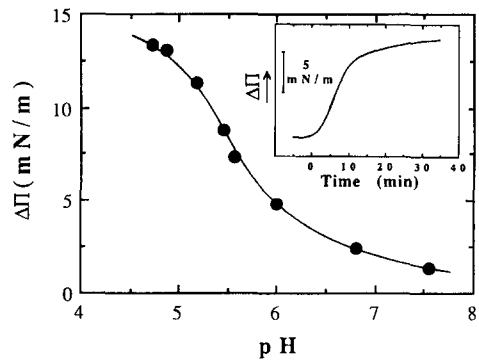

Fig. 2. pH profile of the surface pressure increase ($\Delta\Pi$) induced by 10 μM SFP-1 in the subphase under a DOPC monolayer. The initial surface pressure of the monolayer was 20 mN/m. The curve was drawn through individual points at each pH. Inset: Kinetics of the peptide-induced surface pressure increase (example of kinetics obtained at pH 5.2).

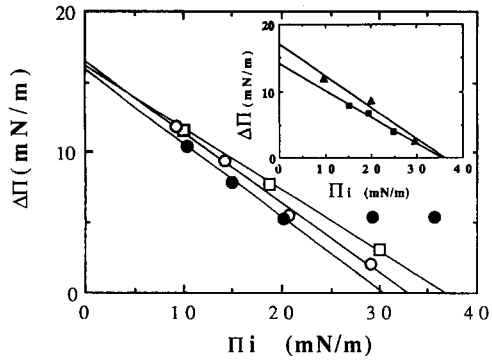

Fig. 3. Dependence of surface pressure increase ($\Delta\Pi$) caused by SFP-1 penetration upon initial surface pressures (Π_i) of phospholipid monolayers at acidic pH. SFP-1 (10 μM) was injected in the subphase at 18°C beneath various phospholipid monolayers: (●) DOPC, (○) bovine brain PS, (□) egg-yolk PE. The inset shows the same experiments after addition of SFP-1 under, respectively, (▲) DOPC/chol (2:1) and (■) DOPC/PS/chol (1:1:1).

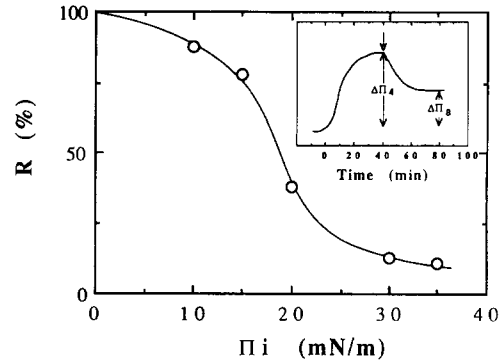

Fig. 4. Percent of SFP-1 desorption after a sharp rise in pH from 4.0 to 8.0 as a function of initial surface pressure (Π_i) of DOPC monolayers. The SFP-1 concentration was 10 μM. The percentage desorption was defined as $R = (\Delta\Pi_4 - \Delta\Pi_8) \times 100/\Delta\Pi_4$ ($\Delta\Pi_4$ and $\Delta\Pi_8$ were defined in the inset). $\Delta\Pi_4$ is the peptide-induced surface pressure change at pH 4.0 and $\Delta\Pi_8$ the corresponding surface pressure variation measured when an equilibrium was established after the sharp rise in pH (arrow). The $\Delta\Pi_8$ values were corrected from the slight effect of the sharp rise in pH on the polar head of DOPC.

peptide was added at acidic pH under a DOPC monolayer. Within approximately 10 min, the peptide-induced increase in surface pressure reached equilibrium (Fig. 2, inset). The pH of the subphase then increased to 8.0. We used the ratio $R = (\Delta\Pi_4 - \Delta\Pi_8) \times 100/\Delta\Pi_4$, with $\Delta\Pi_4$ and $\Delta\Pi_8$ defined in the Fig. 4, inset. This ratio represented the pressure reversion following the pH increase as a function of Π_i. As shown in Fig. 4, a total reversion, i.e., desorption, was observed only for low initial pressure (10 mN/m), with the phenomenon being partially reversible in all other cases. For initial lipid monolayer pressures that are relevant for bilayer membranes (higher than 30 mN/m), pH-induced desorption of SFP-1 was only 10%.

3.3. Peptide secondary structure

We carried out circular dichroism (CD) measurements to determine the secondary structure of SFP-1 at acidic pH. In aqueous solution in the absence of phospholipid vesicles, SFP-1 displayed CD spectra with two minima at 222 and 208 nm corresponding to a random coil conformation. The spectra were measured at pH 7.4, 6.0 and 4.6. Ellipticity at 222 nm (θ_{222}), characteristic for an α-helical conformation, changed from -3300 deg cm^2 dmol^{-1} at pH 7.4 to -14850 deg cm^2 dmol^{-1} at pH 4.6 (Table 1). These results closely agree with those obtained with the longer GALA peptide [16]. The helical content of SFP-1 was considerably greater at pH 4.6 (41%) than at neutral pH (3%), according to the method proposed by Chen et al. [27].

3.4. Peptide destabilizing activity

Since hemolysis is known to be the consequence of erythrocyte membrane destabilization [22,28], we used this assay to follow the destabilizing effect of SFP-1. To mimick the anchored-subunit of fusion peptides, a myristic acid was fixed on the N-terminus of SFP-1. The hemolytic power of SFP-1 was compared with those of the myristoylated peptide (SFP-2) and the myristic acid (MA) used as control. At pH 7.4 (data not shown), no hemolysis of the human erythrocytes was observed. However, at acidic pH (Fig. 5A) the hemolytic power of the myristoylated peptide was 1000-fold higher than that observed with SFP-1 in solution. The hemolysis induced by SFP-2 was not due to the myristic acid. Indeed, 5 μM of SFP-2 totally lysed 10^8 erythrocytes within 10 min (Fig. 5B), while myristic acid did not induce any hemolysis at the same concentration. The destabilizing potential of SFP-1 was thus more important when the peptide hydrophobicity was increased after anchoring it in the cell membrane.

3.5. Peptide fusogenic activity

The fusogenic potency of SFP-3 after coupling to liposomes was studied using the RET between *N*-NBD and *N*-Rh fluorophores. The RET was assessed by an NBD fluorescence decrease (λ_{530}) and concomitant Rh fluorescence increase (λ_{590}) due to the close proximity of the probes, presumably present in the same membrane. No RET was observed with (SFP-3)-coupled liposomes at pH 7.4 (Fig. 6A) as well as with non-(SFP-3)-coupled liposomes at pH 4.5 (Fig. 6B). On the contrary, a rapid RET was noted (Fig. 6C) when (SFP-3)-coupled Rh- and NBD-

Table 1
Ellipticity values (θ_{222}) and helical content of SFP-1 at different pH values

pH	θ_{222} (deg cm^2 dmol^{-1})	Helical content (%)
7.4	−3300	3
6.0	−9900	25
4.6	−14850	41

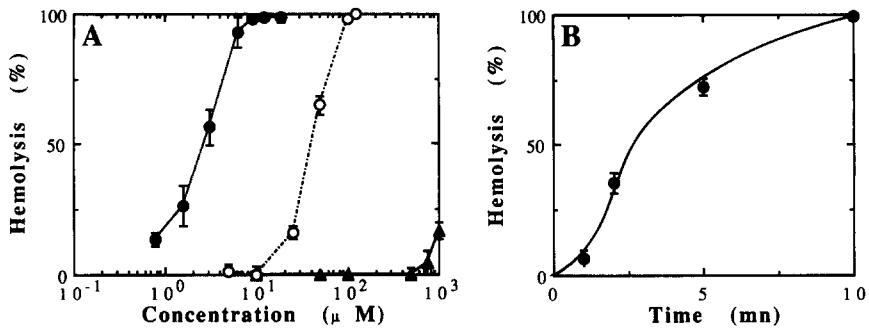

Fig. 5. (A) Dose dependence of SFP-1 (▲), SFP-2 (●) and MA (○) -induced hemolysis. (B) Time dependence of (SFP-2)-induced hemolysis. For details on the experimental procedures see Materials and methods.

labeled liposomes were mixed at pH 4.5. In the inset, the $t_{1/2}$ for the fusion was shown to be about 5 min, leading to 75% fusion yield. Concurrently, laser light scattering measurements showed a marked increase in the vesicle diameters from 235 ± 25 nm at pH 7.4 to 889 ± 57 nm after 30 min at pH 4.5. In these experiments, SFP-3 was coupled to the two liposome preparations. Similar results were obtained with SFP-3 in only one fluorophore-labeled population (data not shown). However, the time-course was then increased ($t_{1/2}$ = 15 min) and the RET intensity was lower (30%). Addition of the same concentration of non-covalently bound SFP-3 to equimolar NBD-PE- and Rh-PE-containing vesicles induced no RET (data not shown).

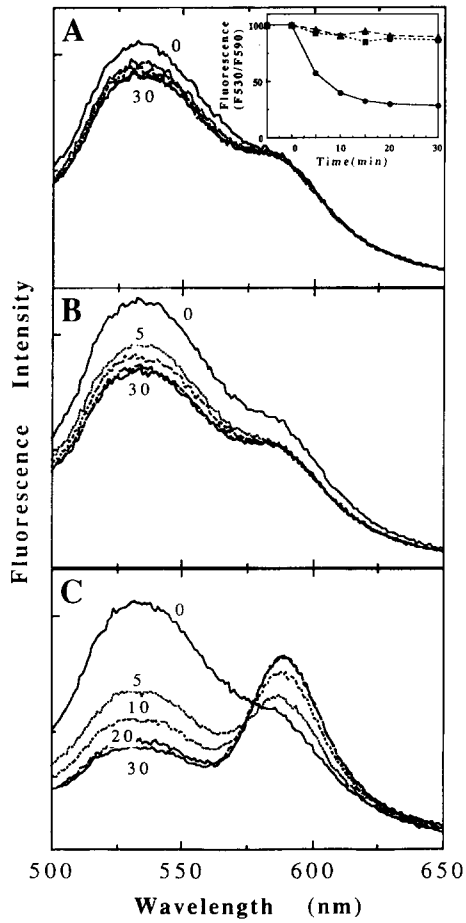

Fig. 6. Time-course of fluorescence emission spectra (λ_{ex} = 470 nm) of an equimolar mixture of NBD-PE- and Rh-PE-containing vesicles (1 mol% fluorescent probe/total lipid). (A) (SFP-3)-coupled liposomes, pH 7.4; (B) non-(SFP-3)-coupled liposomes, pH 4.5; (C) (SFP-3)-coupled liposomes, pH 4.5. Each figure represents the spectra at t = 0, 5, 10, 20 and 30 min. Inset: Time-course of lipid mixing between vesicles. (▲) (SFP-3)-coupled liposomes, pH 7.4; (■) non-(SFP-3)-coupled liposomes, pH 4.5; (●) (SFP-3)-coupled liposomes, pH 4.5. Results were expressed by the F_{530}/F_{590} ratio for each spectrum.

4. Discussion

The aim of this study was to find a short artificial peptide with fusion properties based on common characteristics between viral [6] and model [9,16] fusion peptides. GALA, a 30 amino acid membrane-active peptide, appeared to have a very interesting potential. We therefore synthesized a short GALA-type peptide composed of 14 residues and studied the biophysical and biological properties of this new peptide (SFP) to determine its membrane destabilizing effect and its membrane fusogenic power on a model phospholipid membrane.

As previously suggested, the induction of membrane fusion by a viral fusion protein might involve penetration of the fusion peptide into the target membrane [7,29]. Lipid monolayers have a great potential for studying this kind of pH-dependent protein–lipid interactions [30]. Such experiments clearly demonstrated that SFP-1 became hydrophobic when the pH was lower than 5.5 and it interacted with, and very likely penetrated into, the lipid monolayer with a specific affinity to DOPC (Figs. 2 and 3). This high affinity of SFP-1 to DOPC was only observed with pure monolayers and disappeared with cholesterol. It is well known that cholesterol interacts strongly with PC leading to a specific lateral organization [31] which might hinder particular interactions between SFP-1 and DOPC. The plateau reached a few minutes after the addition of SFP-1 (Fig. 2, inset) is in agreement with previous data on membrane fusion kinetics [32]. Insertion of SFP-1 occurred at surface pressures up to about 32 mN/m, assumed to be the relevant level for lipid monolayers in biological mem-

branes [33–35]. For comparison, the hemagglutinin HA_2 chain N-terminus of the X31 strain of influenza virus, a membrane fusogenic active peptide, has a critical surface pressure for insertion of 34 mN/m [7]. These results closely agree with those obtained by monolayer experiments with several viral fusogenic sequences [7,26], and with the GALA peptide model by tryptophan fluorescence measurements [16].

Several biophysical parameters may modulate interactions between proteins or peptides and lipid monolayers. The most important are Coulombic power and structure of the lipid polar headgroups. For instance, it has been shown that the N-terminus of HIV gp 41 are surface-active and penetrate lipid monolayers composed of negatively charged lipids [10]. Concerning SFP-1, experiments with several lipids (Fig. 3), at different ionic strengths, showed that penetration of SFP-1 did not depend on lipid charge nor on the ionic strength.

Circular dichroism measurements (Table 1) provided good evidence of a pH-induced SFP-1 conformational change. Indeed, the helical content of SFP-1 increased from 3% at pH 7.4 to 41% at pH 4.6. Hence, this sharp rise in pH inducing a SFP-1 conformational change leading to an α-helical structure may be correlated with the lipid interaction and presumably membrane insertion. The increase in monolayer surface pressure is a result of energetically favorable peptide–phospholipid interactions. Moreover, in agreement with well-documented studies, association of the α-helical structure with penetration is consistent with the view that the free energy of transfer of peptide amide groups from water into the apolar bilayer is significantly reduced by the intrapeptide hydrogen-bonding pattern of an α-helix [36].

Recent studies have shown that peptides representing the N-terminal segment of the surface protein gp 41 in two different strains of HIV were α-helical when inserted into monolayers but were in β-sheet conformation when surface-adsorbed [10]. These interesting results were also found by other workers with other hydrophobic signal sequences [37,38]. These authors hypothesize that the inserted α-helical form causes membrane disruption whereas the surface-bound β form induces aggregation. A correlation between the α-helical content and peptide capacity in destabilization of biological membranes has been reported for a number of NHA_2 synthetic analogs [39], gp 41 [10], and other amphipathic peptides [14,40,41]. However, recent monolayer experiments have indicated that a high α-helical content alone is not sufficient to induce fusion activity [26]. The formation of an α-helix may be a prerequisite for membrane destabilization while not guaranteeing that membrane destabilization will occur [11].

Interestingly, irreversibility of the insertion of SFP-1 into a DOPC monolayer (Fig. 4) provides new information on the penetration mechanism. Interaction of SFP-1 with the lipid target is stimulated by lowering the pH (Fig. 2) probably by an irreversible conformational change. At neutral pH, SFP-1 did not interact with the monolayer (Fig. 2). After the peptide conformational change, at monolayer initial surface pressures equivalent to that of the biomembrane leaflet, the pH-increase did not dissociate the peptide from the lipid monolayer (Fig. 4). This suggests that SFP-1 penetrated deeply into the phospholipid leaflet, preventing reversal of the conformational change induced by a sharp rise in pH.

However, a high phospholipid interaction and conformational transition of SFP-1 were not sufficient to induce membrane destabilization. Only a very high SFP-1 concentration (Fig. 5) was able to hemolyse some human erythrocytes in 10 min. Nevertheless, these results closely agree with those obtained by Schlegel and Wade [22], in the same concentration range, on a 25-amino acid peptide corresponding to the NH_2 terminus of the vesicular stomatitis virus G protein. The peptide/lipid mole ratio required for erythrocyte hemolysis was very high (50:1) in comparison to the results (1:500) obtained with GALA on PC vesicle leakage [15,16]. Szoka and coll. have shown that shortening the peptide from 30 to 16 residues decreased the lytic activity of GALA peptides on liposomes by 8-fold [16]. Düzgüneş and Gambale [42] also observed very weak membrane-destabilizing activity of NHA_2 peptides as short as six residues.

We obtained very interesting results showing that the biological effects of SFP-1 could be increased by adding a hydrophobic tail to this peptide. The hemolytic power, predictive of destabilizing potential, of the myristic acid-coupled peptide (SFP-2) was 1000-fold higher than that observed with SFP-1 in solution (Fig. 5A). At least two hypotheses can be advanced to explain this effect. Coupling of the peptide to a membrane might highly reduce hydration forces that represent an important barrier to membrane fusion and/or it could facilitate the α-helix conformational change essential for the fusion process.

Additional experiments using probe mixing assays clearly showed a pH-dependent intermixing of the lipids of the two vesicle populations leading to RET between NBD and Rh and a decrease in the NBD fluorescence signal (Fig. 6). The results of probe mixing assays have to be cautiously interpreted [43]. Indeed, the decrease in the NBD fluorescence can result either from: (i) a probe exchange; (ii) vesicle aggregation; or (iii) an effective membrane fusion between the two vesicle populations. Because of the length of the acyl-chain, the headgroup-labeled analogs, such as NBD-PE and Rh-PE, display an essentially nonexchangeable behavior [44]. Moreover, several arguments suggest a fusion process rather than a mere aggregation: the interactions of SFP with the lipid monolayer, the destabilizing properties of SFP, the range and the kinetics of RET assay and finally the concomitant increase in the vesicle diameters.

Our results are also of a great interest with respect to previous works [6] showing that fusion peptides of viral fusion proteins are always associated with a membrane

segment. This suggests, as noted by Burger et al. [29] with influenza HA_2 peptides, that parts of fusion proteins other than 'fusion peptides' may be involved in the fusion process. On the other hand, we obtained one of the first results showing the effect of membrane-anchoring on the increased destabilizing potential of a synthetic peptide. Indeed, many peptides are known for their fusogenic or destabilizing capacity but until now most were used in solution and only a few have been tested after coupling to liposomes [45].

In conclusion, we showed that a 14-residue GALA-type peptide interacts in a pH-dependent manner with various phospholipids when organized in mono- or bi-layer(s). This interaction is not connected with a Coulombic effect between the peptide and the monolayer, but more related to the peptide conformational change prior to the lipid interaction and layer insertion. SFP is able to destabilize the membrane lipid organization in as much as the peptide is anchored to the membrane. Finally, we have strong presumptions that SFP is fusogenic when coupled to vesicles. It will be of interest to precise the mechanism of SFP-induced fusion, notably by studying other factors influencing the membrane fusion and the concomitant mixing of contents within the two aqueous compartments (in progress in our laboratory). But we feel comforted in our rationale that this short synthetic peptide could be used as a fusion inducer to introduce the aqueous content of a liposomal drug vector into cell cytosol.

Acknowledgements

This work was supported by a grant from l'Agence Nationale de Recherche sur le SIDA (ANRS) and from l'Association pour la Recherche sur le Cancer (ARC). C. Puyal is a recipient of a grant from ANRS. We are grateful to Liliane Leroy (Laboratoire de Physique et Chimie Biomoléculaire, CNRS UA 198, Paris, France), Magali Mezard and Yves Baissac (RSNV, Montpellier, France) for their kind technical assistance with circular dichroism measurements and peptide amino-acid analysis, and to Pierre Milhaud for his critical review of this manuscript.

References

[1] Papahadjopoulos, D., Nir, S. and Düzgüneş, N. (1990) J. Bioenerg. Biomembr. 22, 157–179.
[2] Wilschut, J. (1991) in Membrane Fusion (Wilschut, J. and Hoekstra, D., eds.), pp. 89–126, Marcel Dekker, New York.
[3] Hoekstra, D. (1990) J. Bioenerg. Biomembr. 22, 121–155.
[4] Stegmann, T., Nir, S. and Wilschut, J. (1989) Biochemistry 28, 1698–1704.
[5] White, J.M. (1990) Annu. Rev. Physiol. 52, 679–697.
[6] White, J.M. (1992) Science 258, 917–924.
[7] Rafalski, M., Ortiz, A., Rockwell, A., Van Ginkel, L.C., Lear, J.D., DeGrado, W.F. and Wilschut, J. (1991) Biochemistry 30, 10211–10220.
[8] Stegmann, T., Delfino, J.M., Richards, F.M. and Helenius, A. (1991) J. Biol. Chem. 266, 18404–18410.
[9] Kono, K., Kimura, S. and Imanishi, Y. (1990) Biochemistry 29, 3631–3637.
[10] Rafalski, M., Lear, J.D. and DeGrado, W.F. (1990) Biochemistry 29, 7917–7922.
[11] Gallaher, W.R., Segrest, J.P. and Hunter, E. (1992) Cell 70, 531–532.
[12] Compagnon, B., Milhaud, P., Bienvenüe, A. and Philippot, J.R. (1992) Exp. Cell Res. 200, 333–338.
[13] Earl, R.T., Billet, E.E., Hunneyball, I.M. and Mayer, R.J. (1987) Biochem. J. 241, 801–807.
[14] Parente, R.A., Nir, S. and Szoka, F.C., Jr. (1988) J. Biol. Chem. 10, 4724–4730.
[15] Parente, R.A., Nadasdi, L., Subbarao, N.K. and Szoka, F.C., Jr. (1990) Biochemistry 29, 8713–8719.
[16] Subbarao, N.K., Parente, R.A., Szoka, F.C., Jr., Nadasdi, L. and Pongracz, K. (1987) Biochemistry 26, 2964–2972.
[17] Lowry, O.H., Rosebrough, N.J. and Randall, R.L. (1951) J. Biol. Chem. 193, 265–275.
[18] Gaines, G.L. (1966) in Insoluble Monolayers at Liquid Gas Interfaces, Wiley-Interscience, New York.
[19] Seta, P., Bienvenüe, E., d'Epenoux, B., Tenebre, L. and Momenteau, M. (1987) Photochem. Photobiol. 45, 137–142.
[20] Kaiser, E.T. and Kezdy, F.J. (1984) Science 223, 249–255.
[21] Lee, S., Mihara, H., Aoyagi, H., Kato, T., Izumiya, N. and Yamasaki, N. (1986) Biochim. Biophys. Acta 862, 211–219.
[22] Schlegel, R. and Wade, M. (1984) J. Biol. Chem. 259, 4691–4694.
[23] New, R.R.C. (1990) in Liposomes a Practical Approach, Oxford University Press.
[24] Bartlett, G.R. (1959) J. Biol. Chem. 234, 466–468.
[25] Hoekstra, D. (1982) Biochemistry 21, 2833–2835.
[26] Burger, K.N.J., Wharton, S.A., Demel, R.A. and Verkleij, A.J. (1991) Biochemistry 30, 11173–11180.
[27] Chen, Y.H., Yang, J.T. and Martinez, H.M. (1972) Biochemistry 11, 4120–4131.
[28] Wilde, A., McQuain, C. and Morrison, T. (1986) Virus Res. 5, 77–95.
[29] Burger, K.N.J., Wharton, S.A., Demel, R.A. and Verkleij, A.J. (1991) Biochim. Biophys. Acta 1065, 121–129.
[30] Pattus, F., Martinez, M.C., Dargent, B., Cavard, D., Verger, R. and Lazdunski, C. (1983) Biochemistry 22, 5698–5703.
[31] Chapman, D. (1973) in Form and Function of Phospholipids (Ansell, G.B., Dawson, R.M.C. and Hawthorne, J.N., eds.), pp. 117–141, Elsevier/North-Holland, Amsterdam.
[32] Stegmann, T., Hoekstra, D., Scherphof, D. and Wilschut, J. (1986) J. Biol. Chem. 261, 10966–10969.
[33] Demel, R.A. and De Kruijff, B. (1976) Biochim. Biophys. Acta 457, 109–132.
[34] Blume, A. (1979) Biochim. Biophys. Acta 557, 32–44.
[35] Seelig, A. (1987) Biochim. Biophys. Acta 899, 196–204.
[36] Roseman, M.A. (1988) J. Mol. Biol. 201, 621–623.
[37] Batenburg, A.M., Demel, R.A., Verkleij, A.J. and De Kruijff, B. (1988) Biochemistry 27, 5678–5685.
[38] Cornell, D.G. and Dluhy, R.A. (1989) Biochemistry 28, 2789–2797.
[39] Wharton, S.A., Martin, S.R., Ruigrok, R.W.H., Skehel, J.J. and Wiley, D.C. (1988) J. Gen. Virol. 69, 1847–1857.
[40] Keller, R.C.A., Killian, J.A. and De Kruijf, B. (1992) Biochemistry 31, 1672–1677.
[41] Yoshimura, T., Goto, Y. and Aimoto, S. (1992) Biochemistry 31, 6119–6126.
[42] Düzgüneş, N. and Gambale, F. (1988) FEBS Lett. 227, 110–114.
[43] Düzgüneş, N., Allen, T.M., Fedor, J. and Papahadjopoulos, D. (1987) Biochemistry 26, 8435–8442.
[44] Nichols, J.W. and Pagano, R.E. (1983) J. Biol. Chem. 258, 5368–5372.
[45] Kato, T., Lee, S., Ono, S., Agawa, Y., Aoyagi, H., Ohno, M. and Nishino, N. (1991) Biochim. Biophys. Acta 1063, 191–196.